

**CATALYTIC PYROLYSIS OF WASTE TIRE OVER HMOR-BASED  
CATALYSTS: INDUSTRIALIZED Ru/HMOR-BASED CATALYST**

Palida Sritana

A Thesis Submitted in Partial Fulfilment of the Requirements  
for the Degree of Master of Science  
The Petroleum and Petrochemical College, Chulalongkorn University  
in Academic Partnership with  
The University of Michigan, The University of Oklahoma,  
and Case Western Reserve University

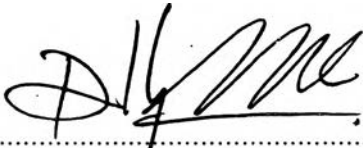
2010

I 28375439

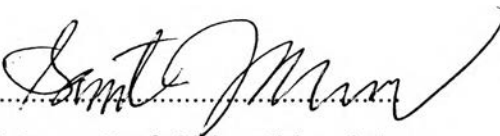
**Thesis Title:** Catalytic Pyrolysis of Waste Tire over HMOR-based Catalysts: Industrialized Ru/HMOR-based Catalyst  
**By:** Palida Sritana  
**Program:** Petrochemical Technology  
**Thesis Advisor:** Assoc. Prof. Sirirat Jitkarnka

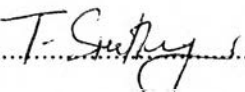
---

Accepted by the Petroleum and Petrochemical College, Chulalongkorn University, in partial fulfilment of the requirements for the Degree of Master of Science.

  
..... Dean  
(Asst. Prof./Pomthong Malakul)

**Thesis Committee:**

  
.....  
(Assoc. Prof. Sirirat Jitkarnka)

  
.....  
(Asst. Prof. Thammanon Sreethawong)

  
.....  
(Dr. Natthakorn Kraikul)

## ABSTRACT

5171014063: Petrochemical Technology Program

Palida Sritana: Catalytic Pyrolysis of Waste Tire over HMOR-based

Catalysts: Industrialized Ru/HMOR-based Catalyst

Thesis Advisors: Assoc. Prof. Sirirat Jitkarnka 134 pp.

Keywords: Pyrolysis / Waste tires / Light olefins / Ruthenium / HMOR /

Bifunctional catalysts / Matrix

The catalytic pyrolysis of waste tire has been studied in this research. The goal was to develop the Ru-supported HMOR catalyst as an industrial catalyst for the production of light olefins (ethylene and propylene) in the gaseous product from the catalytic pyrolysis of waste tires. The catalysts consist of the Ru/HMOR zeolite (active), a clay (matrix), and an  $\alpha$ -alumina (binder). The optimum composition of the Ru/HMOR-based catalyst was determined, and the effect of ratio of pellet diameter to reactor diameter, and the deactivation of the catalyst by coking were investigated for their influences on the quality and quantity of pyrolysis products, especially the light olefins in the gaseous product. As a result, the optimum composition of the catalyst for light olefins and naphtha production was 20 %wt of Ru/HMOR, 70 %wt of kaolin, and 10 %wt of  $\alpha$ -alumina. The matrix was found to help the heat dissipation during reaction. The influence of pellet diameter was on the diffusion limitation in the solid catalyst. The best ratio of pellet to reactor diameter for the maximum light olefins production was 0.0556 (3.0 mm of pellet diameter) for the bench-scale autoclave reactor. In addition, the deactivation of the catalyst was caused by the coke formation, the sulphur deposition, and the metal agglomeration.

## บทคัดย่อ

ปาติดา ศรีธนะ: การไพโรไลซิสของยางหมดสภาพด้วยตัวเร่งปฏิกิริยามอร์ดีไนท์ซีโอไลท์: การพัฒนาตัวเร่งปฏิกิริยาที่นิยมบนมอร์ดีไนท์ซีโอไลท์เพื่ออุตสาหกรรม (Catalytic Pyrolysis of Waste Tires over HMOR-based Catalysts: Industrialized Ru/HMOR-based Catalyst) อ. ที่ปริกษา รศ. ดร. ศิริรัตน์ จิตการคำ 134 หน้า

งานวิจัยนี้เป็นงานวิจัยที่ศึกษาเกี่ยวกับกระบวนการไพโรไลซิสยางหมดสภาพ โดยมีจุดมุ่งหมายคือ การพัฒนาตัวเร่งปฏิกิริยาที่นิยมบนมอร์ดีไนท์ เพื่ออุตสาหกรรมการผลิตสารประกอบโอเลฟินส์เบา เช่น เอทิลีน และ โพรพิลีน ในผลผลิตที่เป็นก๊าซจากกระบวนการไพโรไลซิสยางหมดสภาพ ตัวเร่งปฏิกิริยาดังกล่าวประกอบด้วยรูทีเนียมบนมอร์ดีไนท์ (ตัวรองรับ), ดินเหนียว (ตัวรองรับ) และ แอลฟาอะลูมินา (ตัวประสาน) ในงานวิจัยได้ศึกษาหาส่วนประกอบที่เหมาะสมของตัวเร่งปฏิกิริยา, ผลของอัตราส่วนระหว่างเส้นผ่านศูนย์กลางของตัวเร่งปฏิกิริยากับเส้นผ่านศูนย์กลางของปฏิกรณ์ และการเสื่อมสภาพของตัวเร่งปฏิกิริยาจากการเกิดถ่านโค้ก ที่จะมีผลต่อคุณภาพและปริมาณของผลผลิตที่ได้จากการไพโรไลซิส ผลปรากฏว่าตัวเร่งปฏิกิริยาที่ดีที่สุดจะต้องมีองค์ประกอบดังต่อไปนี้ คือ รูทีเนียมบนมอร์ดีไนท์ร้อยละ 20 ดินเหนียวร้อยละ 70 และแอลฟาอะลูมินาร้อยละ 10 จากนั้นพบว่า ตัวรองรับจะช่วยในการกระจายความร้อนในขณะการเกิดปฏิกิริยา สำหรับปฏิกรณ์ประเภทอโตเคลฟแบบตั้งโต๊ะ การเปลี่ยนแปลงขนาดเส้นผ่านศูนย์กลางของตัวเร่งปฏิกิริยามีผลทำให้การแพร่ของสารตั้งต้นในตัวเร่งปฏิกิริยามีข้อจำกัด ซึ่งพบว่า ปริมาณโอเลฟินส์เบาถูกผลิตได้สูงสุดที่อัตราส่วนระหว่างเส้นผ่านศูนย์กลางของตัวเร่งปฏิกิริยากับปฏิกรณ์ เท่ากับ 0.0556 (เส้นผ่านศูนย์กลางของตัวเร่งปฏิกิริยาเท่ากับ 3 มิลลิเมตร) นอกจากนี้พบว่าการเสื่อมสภาพของตัวเร่งปฏิกิริยานั้นเกิดจากสาเหตุดังนี้ คือ การเกิดถ่านโค้กบนตัวเร่งปฏิกิริยา การเกิดการสะสมของกำมะถันบนตัวเร่งปฏิกิริยา และการรวมตัวกันของโลหะบนตัวเร่งปฏิกิริยา

## ACKNOWLEDGEMENTS

This thesis could not have been complete without the assistance and support of my advisor, college and my family.

I would like to deep indebted to Assoc. Prof. Sirirat Jitkarnka, my advisor, who provided the suggestions, useful recommendation, valuable support, and encouragement throughout this research work.

I am grateful for the scholarship and funds provided by the Petroleum and Petrochemical College, Thailand Researched Fund, the Commissions on Higher Education, and the National Center of Excellence for Petroleum, Petrochemicals, and Advanced Materials, Thailand.

Special thanks are given to Dr. Nguyen Anh Dung, a former Ph.D. student, for his valuable suggestions, comments, and encouragement.

Special recognition is forwarded to all The Petroleum and Petrochemical College's staff for the helps in fixing analytical instruments, valuable suggestions on characterization instruments and other useful helps in this study.

Finally, I would like to thank all of my friends and PhD students for their friendly cheerful, creative suggestions and useful assistance. Also, I would like to gratitude to my parents and my sister for their care, love, and understanding all supports to me all the time.

**TABLE OF CONTENTS**

	<b>PAGE</b>
Title Page	i
Abstract (in English)	iii
Abstract (in Thai)	iv
Acknowledgements	v
Table of Contents	vi
List of Tables	ix
List of Figures	xiv
 <b>CHAPTER</b>	
<b>I INTRODUCTION</b>	<b>1</b>
<b>II LITERATURE REVIEW</b>	<b>4</b>
<b>III EXPERIMENTAL</b>	<b>13</b>
3.1 Materials	13
3.2 Equipment	14
3.3 Chemicals and solvents	14
3.4 Methodology	15
3.4.1 Catalyst preparation	15
3.4.2 Reaction equipment	16
3.4.3 Catalyst characterization	17
3.4.4 Oil analysis	19
3.4.5 Gas analysis	21

<b>CHAPTER</b>	<b>PAGE</b>
<b>VI RESULTS AND DISCUSSION</b>	22
4.1 Determination of the optimum component of a commercial Ru/HMOR-based catalyst	22
4.1.1 Catalyst characterization	22
4.1.2 Product Distribution	26
4.1.3 Gas Yields	27
4.1.4 Light Olefins Production	28
4.1.5 Liquid analysis	31
4.1.5.1 Petroleum Fraction Analysis	31
4.1.5.2 Asphaltenes	33
4.1.6 Spent Catalyst Characterization	36
4.2 Effect of Ratio of $D_{\text{pellet}}$ to $D_{\text{reactor}}$	39
4.2.1 Pyrolysis products	40
4.2.2 Quality of Pyrolysis Products	43
4.3 Deactivation of catalyst by coking	51
4.3.1 Catalyst characterization	51
4.3.2 Pyrolysis products	55
<b>V CONCLUSIONS AND RECOMMENDATIONS</b>	62
<b>REFERENCES</b>	63
<b>APPENDICES</b>	68
<b>Appendix A</b> Operating Temperature	68
<b>Appendix B</b> Yields of Pyrolysis Products	84

<b>CHAPTER</b>	<b>PAGE</b>
<b>Appendix C</b> The Pyrolysis Gas Compositions	85
<b>Appendix D</b> Amount of Asphaltene in Pyrolysis Oil	87
<b>Appendix E</b> Chemical Compositions of Maltenes	88
<b>Appendix F</b> True Boiling Point of Maltenes	90
<b>Appendix G</b> True Boiling Point of Maltenes, Saturated Hydrocarbons, Mono-, Di-, Poly-, and Polar- Aromatics in Maltenes	94
<b>Appendix H</b> Carbon Number Distributions	110
<b>Appendix I</b> Petroleum Fraction of Derived Oils	129
<b>Appendix J</b> Effectiveness Factor Calculations	131
<b>Appendix K</b> Metal Dispersion Calculations	132
<b>Appendix L</b> Mean Particle Size Calculation from Dispersion	133
<b>CURRICULUM VITAE</b>	134



## LIST OF TABLES

TABLE		PAGE
2.1	Varied compositions of a being-developed catalyst	11
3.1	Elemental composition of waste tire (Dũng et al., 2009)	13
3.2	Chemical compositions of kaolin	13
3.3	The optimized compositions and volumes of mobile phases for preparative separation of petroleum maltenes using the chromatographic column (Sebor <i>et al.</i> , 1999)	20
4.1	Physical and chemical properties of the studied Ru/HMOR-based catalysts	23
4.2	Thermal conductivity of the studied Ru/HMOR-based catalysts	30
4.3	The boiling point and carbon ranges of refinery products (Nguyễn et al., 2010)	32
4.4	Coke and sulfur in the spent catalysts	37
4.5	Physical properties of the fresh catalysts and the coke and sulfur contents in the spent catalysts	39
4.6	The effectiveness factors of each pellet diameter	50
4.7	Physical properties of the regenerated catalysts	53
4.8	Coke and sulfur contents in the spent catalysts	53
A1	Operating temperatures: Batch 1 (no Cat): 22-07-2009	68
A2	Operating temperatures: Batch 2 (HMOR): 29-07-2009	69
A3	Operating temperatures: Batch 3 (Ru/HMOR): 30-07-2009	70
A4	Operating temperatures: Batch 4 (Kaolin): 31-07-2009	71
A5	Operating temperatures: Batch 5 (Alumina): 03-08-2009	72
A6	Operating temperatures: Batch 6 (BC-20): 06-08-2009	73
A7	Operating temperatures: Batch 7 (BC-30): 07-08-2009	74

<b>TABLE</b>	<b>PAGE</b>
A8 Operating temperatures: Batch 8 (BC-40): 16-08-2009	75
A9 Operating temperatures: Batch 9 (BC-50): 17-08-2009	76
A10 Operating temperatures: Batch 10 (Pellet diameter 1.00mm): 14-09-2009	77
A11 Operating temperatures :Batch 11 (Pellet diameter 2.00mm): 17-09-2009	78
A12 Operating temperatures :Batch 12 (Pellet diameter 3.00mm): 06-10-2009	79
A13 Operating temperatures :Batch 13 (Pellet diameter 4.00mm): 12-10-2009	80
A14 Operating temperatures :Batch 14 (Flash Cat.): 06-10-2009	81
A15 Operating temperatures :Batch 15 (Spent Cat.1): 23-10-2009	82
A16 Operating temperatures :Batch 16 (Spent Cat.2): 27-10-2009	83
B1 Weight percentage of pyrolysis products obtained from each separate component in the Ru/HMOR based catalysts	84
B2 Weight percentage of pyrolysis products obtained from the Ru/HMOR based catalysts	84
B3 Weight percentage of pyrolysis products obtained from the BC-20 catalyst with various pellet diameters	84
B4 Weight percentage of pyrolysis products from the catalyst deactivation testing	85
C1 Weight percentage of gas product obtained from each separate component in the Ru/HMOR based catalysts	85
C2 Weight percentage of gas product obtained from the Ru/HMOR based catalysts	86
C3 Weight percentage of gas products obtained from the BC-20 catalyst with various pellet diameters	86

<b>TABLE</b>	<b>PAGE</b>
C4 Weight percentage of gas products from the catalyst deactivation testing	87
D1 Amount of asphaltene in pyrolysis oil	87
E1 Chemical compositions of maltenes obtained from each separate component in the Ru/HMOR based catalysts	88
E2 Chemical compositions of maltenes obtained from the Ru/HMOR based catalysts	88
E3 Chemical compositions of maltenes obtained from the BC-20 catalyst with various pellet diameters	88
E4 Chemical compositions of maltenes from the catalyst deactivation testing	89
F1 True boiling point of maltenes obtained from each separate component in the Ru/HMOR based catalyst	90
F2 True boiling point of maltenes obtained from the Ru/HMOR based catalysts	91
F3 True boiling point of maltenes obtained from the BC-20 catalyst with various pellet diameters	92
F4 True boiling point of maltenes from the catalyst deactivation testing	93
G1 Batch 1 (no Cat)	94
G2 Batch 2 (HMOR)	95
G3 Batch 3 (Ru/HMOR)	96
G4 Batch 4 (Kaolin)	97
G5 Batch 5 (Alumina)	98
G6 Batch 6 (BC-20)	99
G7 Batch7 (BC-30)	100
G8 Batch8 (BC-40)	101
G9 Batch9 (BC-50)	102

<b>TABLE</b>	<b>PAGE</b>
G10 Batch 10 (Pellet diameter 1.00mm)	103
G11 Batch 11 (Pellet diameter 2.00mm)	104
G12 Batch 12 (Pellet diameter 3.00mm)	105
G13 Batch 13 (Pellet diameter 4.00mm)	106
G14 Batch 14 (Flash Cat.)	107
G15 Batch 15 (Spent Cat.1)	108
G16 Batch 16 (Spent Cat.2)	109
H1 Carbon number distribution of maltenes obtained from each separate component in the Ru/HMOR based catalysts	110
H2 Carbon number distribution of maltenes obtained from the Ru/HMOR based catalysts	111
H3 Carbon number distribution of maltenes obtained from the BC-20 catalyst with various pellet diameters	112
H4 Carbon number distribution of maltenes from the catalyst deactivation testing	113
H5 Carbon number distribution of saturated hydrocarbons obtained from the Ru/HMOR based catalysts	114
H6 Carbon number distribution of saturated hydrocarbons obtained from the BC-20 catalyst with various pellet diameters	115
H7 Carbon number distribution of saturated hydrocarbons from the catalyst deactivation testing	116
H8 Carbon number distribution of mono-aromatics obtained from the Ru/HMOR based catalysts	117
H9 Carbon number distribution of mono-aromatics obtained from the BC-20 catalyst with various pellet diameters	118
H10 Carbon number distribution of mono-aromatics from the catalyst deactivation testing	119

<b>TABLE</b>		<b>PAGE</b>
H11	Carbon number distribution of di-aromatics obtained from the Ru/HMOR based catalysts	120
H12	Carbon number distribution of di-aromatics obtained from the BC-20 catalyst with various pellet diameters	121
H13	Carbon number distribution of di-aromatics from the catalyst deactivation testing	122
H14	Carbon number distribution of poly-aromatics obtained from the Ru/HMOR based catalysts	123
H15	Carbon number distribution of poly-aromatics obtained from the BC-20 catalyst with various pellet diameters	124
H16	Carbon number distribution of poly-aromatics from the catalyst deactivation testing	125
H17	Carbon number distribution of polar-aromatics obtained from the Ru/HMOR based catalysts	126
H18	Carbon number distribution of polar-aromatics obtained from the BC-20 catalyst with various pellet diameters	127
H19	Carbon number distribution of polar-aromatics from the catalyst deactivation testing	128
I1	Petroleum fractions of derived oils obtained from each separate component in Ru/HMOR based catalysts	129
I2	Petroleum fractions of derived oils obtained from the Ru/HMOR based catalysts	129
I3	Petroleum fractions of derived oils obtained from the BC-20 catalyst with various pellet diameters	129
I4	Petroleum fractions of derived oils from the catalyst deactivation testing	130

**LIST OF FIGURES**

<b>FIGURE</b>		<b>PAGE</b>
2.1	Pathways for the formation of monomer and dimer components from polyisoprene rubbers by pyrolysis (Sato <i>et al.</i> , 2003).	5
2.2	Possible mode of degradation of polybutadiene (Uhl <i>et al.</i> , 2000).	6
2.3	Styrene-Butadiene bond dissociation (Choi, 2000).	7
2.4	Flowchart of step in the study on catalyst deactivation by coke formation.	12
3.1	Schematic of experimental pyrolysis system (Dũng <i>et al.</i> , 2009).	17
4.1	Variation of the pore size distribution of the studied Ru/HMOR-based catalysts and each separate component.	24
4.2	The XRD patterns of: (a) $\alpha$ -alumina, (b) kaolin, (c) BC-20, (d) BC-30, (e) BC-40, (f) BC-50, and (g) Ru/HMOR.	25
4.3	An appearance of the studied Ru/HMOR-based catalysts with various compositions.	26
4.4	Product distributions from the catalytic pyrolysis of scrap tire using the Ru/HMOR-based catalysts with various compositions.	26
4.5	Gas compositions from the catalytic pyrolysis of scrap tire using the Ru/HMOR-based catalysts with various compositions.	28
4.6	Light olefins production from the catalytic pyrolysis of scrap tire using the Ru/HMOR-based catalysts with various compositions.	29

<b>FIGURE</b>		<b>PAGE</b>
4.7	Light olefins production per kilogram of tire and gram of active Ru/HMOR.	31
4.8	Petroleum Fractions in maltenes obtained from the catalytic pyrolysis of scrap tire using the Ru/HMOR-based catalysts with various compositions.	32
4.9	Naphtha production per kilogram of tire and gram of active Ru/HMOR.	33
4.10	Weight percentage of asphaltene in pyrolytic oils obtained from the catalytic pyrolysis of scrap tire using the Ru/HMOR-based catalysts with various compositions.	34
4.11	Chemical compositions in maltenes obtained from the catalytic pyrolysis of scrap tire using the Ru/HMOR-based catalysts with various compositions: (a) the ratio of saturated hydrocarbons to total aromatic hydrocarbons, and (b) the ratio of mono aromatic to total aromatic hydrocarbons.	35
4.12	Sulfur content in pyrolytic oils obtained from the catalytic pyrolysis of scrap tire using the Ru/HMOR-based catalysts with various compositions.	36
4.13	The TG results of the studied Ru/HMOR-based catalysts.	37
4.14	An appearance of the studied Ru/HMOR-based catalysts with various pellet diameters.	40
4.15	Gas to liquid ratio obtained from the catalytic pyrolysis of scrap tire using the BC-20 catalyst with various ratios of pellet diameter to reactor diameter.	40
4.16	Light olefins production obtained from the catalytic pyrolysis of scrap tire using the BC-20 catalyst with various ratios of pellet diameter to reactor diameter.	41

<b>FIGURE</b>	<b>PAGE</b>
4.17 Petroleum Fractions in maltenes obtained from the catalytic pyrolysis of scrap tire using the BC-20 catalyst with various ratios of pellet diameter to reactor diameter: (a) weight percentage, and (b) yield per kg. of tire.	42
4.18 Weight percentage of asphaltene in the pyrolytic oils obtained from the catalytic pyrolysis of scrap tire using the BC-20 catalyst with various ratios of pellet diameters to reactor diameters.	44
4.19 The ratio of saturated hydrocarbons to total aromatics in the maltenes obtained from the catalytic pyrolysis of scrap tire using the BC-20 catalyst with various ratios of pellet diameter to reactor diameter.	44
4.20 The ratio of mono-aromatic to total aromatics in the maltenes obtained from the catalytic pyrolysis of scrap tire using the BC-20 catalyst with various ratios of pellet diameter to reactor diameter.	45
4.21 Sulfur in the pyrolytic oils obtained from the catalytic pyrolysis of scrap tire using the BC-20 catalyst with various ratios of pellet diameter to reactor diameter.	45
4.22 Concentration profile of a reacting species in the vicinity of a porous catalyst particle (Davis <i>et al.</i> , 2003).	46
4.23 Effectiveness factor $[\eta = \frac{\tanh(\phi)}{\phi}]$ for a first-order reaction in a catalyst as a function of the Thiele modulus with generalized length parameter (Davis <i>et al.</i> , 2003).	47
4.24 Scheme of a cylindrical catalyst particle (Davis <i>et al.</i> , 2003).	49
4.25 The XRD patterns of the catalysts.	52



<b>FIGURE</b>		<b>PAGE</b>
4.26	Variation of the pore sizes of the regenerated catalysts.	54
4.27	Relationship between the wt% coke deposition and the number of cycle.	55
4.28	Gas to liquid ratio obtained from 1 to 3 cycles of operations.	56
4.29	Yields of gas compositions obtained from 1 to 3 cycles of operations.	57
4.30	Yields of ethylene, propylene, and light olefins obtained from 1 to 3 cycles of operations.	57
4.31	Petroleum fractions in the maltenes obtained from 1 to 3 cycles of operations.	58
4.32	Weight percentage of asphaltene in pyrolytic oils obtained from 1 to 3 cycles of operations.	59
4.33	The ratio of saturated hydrocarbons to total aromatics in the maltenes obtained from 1 to 3 cycles of operations.	60
4.34	The ratio of mono-aromatic to total aromatics in the maltenes obtained from 1 to 3 cycles of operations.	60
4.35	Sulfur in the pyrolytic oils obtained from 1 to 3 cycles of operations.	61